Available online at www.sciencedirect.com
ScienceDirect
Procedia Environmental Sciences 20 (2014) 642 – 650
Procedia Environmental Sciences

The 4th International Conference on Sustainable Future for Human Security, SustaiN 2013

Study on Reducing Tsunami Inundation Energy by the Modification of Topography Based on Local Wisdom

Fadly Usman[a,c,*], Keisuke Murakami[b], Eddi Basuki Kurniawan[c]

[a]*Interdisciplinary Graduate School of Agriculture and Engineering, 1-1 Gakuen Kibanadai Nishi, Miyazaki, 889-2192, Japan*
[b]*Dept. of Civil and Environmental Engineering, University of Miyazaki, 1-1 Gakuen Kibanadai Nishi, Miyazaki 889-2192, Japan*
[c]*Department of Urban and Regional Planning, Brawijaya University, MT Haryono 167, Malang, 65145, Indonesia*

Abstract

The effective use of those local wisdoms is strongly desired, especially in developing countries, because it is quite difficult for those countries to allocate enough budgets for constructing hard-type countermeasures against tsunami. Among local wisdoms against tsunami hazard, this study evaluated the efficiency of a hollow topography which can be seen on the beach along Lampon village in Indonesia. These artificial hollows are arrayed on the beach as one of the local wisdoms in Lampon village to reduce the intensity of inundated tsunami flow. The numerical simulation of tsunami inundation energy was conducted to evaluate the efficiency of this hollow topography. In order to investigate the effect of artificial topography and vegetation belt, this study conducted a numerical simulation utilizing CADMAS-SURF 3D. Furthermore, this study evaluated the efficiency of some contrivances, such as combination of vegetation belts and a multiple-use of hollow and embankment topography, in order to enhance the performance of a countermeasure based on the local wisdom.

Selection and peer-review under responsibility of the SustaiN conference committee and supported by Kyoto University; (RISH), (OPIR), (GCOE-ARS) and (GSS) as co-hosts

Keywords: Tsunami; Local wisdom; Numerical simulation; CADMAS SURF 3D

* Corresponding author. Tel.: +81-804279-4912, +62-812-32-553923
E-mail address: fadlypwk@ub.ac.id, fadlypwkftub@gmail.com

Selection and peer-review under responsibility of the SustaiN conference committee and supported by Kyoto University; (RISH), (OPIR), (GCOE-ARS) and (GSS) as co-hosts
doi:10.1016/j.proenv.2014.03.077

1. Introduction

The aim of this study was to investigate tsunami disaster mitigation with the approach of local wisdom in Indonesia. There are a lot of local wisdoms as soft-type measures or hard-type ones to mitigate tsunami damages. Some of those wisdoms seemed to be useful under the limited budget for disaster prevention strategy in developing countries, and the effect of local wisdoms should be evaluated technically. Among local wisdoms to encounter tsunami hazard, the effect of topography modification that can be seen on the beach along Lampon village was evaluated in this study.

The relatively low death toll on the Indonesian island of Simeuleu, which is close to the earthquake's epicenter, has been attributed partly to the surrounding mangrove forests and their local wisdom. Yanagisawa et al. (2009) reported their research techniques within their site survey analysis and produced analytical results. They showed that with a 400m forest width, 26% of the inundation depth was reduced while a 1.000m of forest width would reduce about 45% of the inundation depth at a maximum current velocity of 5 m/s and tsunami heights between 4 and 8 m [1].

On March 11, 2011, Great East Japan Tsunami discovered that the pine tree forests in Rikuzentakata, Iwate unfortunately could not prevent or reduce the tsunami energy. This means that there is a limit of the performance of coastal vegetation against tsunami of this size. However, mangrove forests are entirely dissimilar to pine trees in terms of the vegetation physical characteristics and anatomy [2]. At beach forests, sufficient forest width is necessary to absorb enough tsunami's energy to reduce flow velocity and depth before exiting the forest. In West Java of Indonesia, for example, 40 meters of beach forest were effective in reducing tsunami of 6-7 meter waves to just 1.6 meters in 2006 [3]. In Sri Lanka, *Pandanus sp* and *Cocus nucifera sp* reduced the 2004 tsunami of 100 meters to 4.5-5.5 meters wave [4], and elsewhere of 155 meters to 6.0 meter wave [5].

Lampon village in Banyuwangi on Java Island experienced an earthquake with magnitude of 7.6 in 1994. A sizeable tsunami hit this coast 50 minutes after the main shock. The tsunami height in Lampon village was measured of 5.4m. On the other hand, 9.1m tsunami height was also measured at another point on the seaside for about 1km east of the village [6]. Between these two points, there is a vegetation area and an artificial hollowed area. When earthquake occured, those topographic features might reduce the tsunami energy in Lampon village.

An aerial photo in Fig.1.a introduces a typical coastal area in Lampon village, Banyuwangi, Indonesia. A vegetation area and a hollow topography can be seen in this photo. There are some artificial hollows on this beach with the size of 100m in length, 20m in width and 2m in depth. Fig.1.b shows another type of coastal area in Southern Java Island which is Telengria beach, Pacitan. There are sand dunes, grass area and vegetation area on this beach with the sand dune of about 60m in width, grass area of 50m and vegetation area of about 75m in width.

Fig. 1(a) Typical coastal area in Lampon village, Banyuwangi; (b) Typical coastal area in Telengria beach, Pacitan.

This study evaluates the efficiency and the effectiveness of the topography modification in reducing tsunami inundation depth and velocity. Two-dimensional numerical analysis is conducted in this study to investigate the inundation flow over the hollow topography. Furthermore, this study evaluates the efficiency of some contrivances, such as combination of vegetation area, multiple uses of hollow and embankment topography in order to enhance the performance of countermeasure based on the local wisdom.

2. Methodology

Numerical analysis was conducted to analyze several types of beach topographies and configurations in this study. This study employs CADMAS-SURF/3D to conduct a numerical simulation. The basic equations in this direct numerical simulation are the continuity equation and momentum equation, known as the Navier-Stokes equations. This study employs a system of such equations, discretized with the finite difference method to simulate tsunami flow around three-dimensional obstacles on topography.

2.1. Numerical Simulation Method

The governing equations used in this study are continuity equation expressed in Eq. (1) and momentum equation from Eq. (2) to Eq. (4). This system of equations was proposed by Sakakiyama and Kajima (1992) [7], where the area porosities γ_x, γ_y, γ_y in x, y and z projections were introduced in order to investigate the interaction between waves and the modification of topography.

$$\frac{\partial \gamma_x u}{\partial x} + \frac{\partial \gamma_z v}{\partial y} + \frac{\partial \gamma_z w}{\partial z} = S_p \tag{1}$$

$$\lambda_v \frac{\partial u}{\partial t} + \frac{\partial \lambda_x uu}{\partial x} + \frac{\partial \lambda_y vu}{\partial y} + \frac{\partial \lambda_z wu}{\partial z} = -\frac{\gamma_v}{\rho}\frac{\partial p}{\partial x} + \frac{\partial}{\partial x}\left\{\gamma_x v_e \left(2\frac{\partial u}{\partial x}\right)\right\} \tag{2}$$

$$+\frac{\partial}{\partial z}\left\{\gamma_z v_e \left(\frac{\partial u}{\partial z} + \frac{\partial w}{\partial x}\right)\right\} - \gamma_v D_x u - R_x + \gamma_v S_u$$

$$\lambda_v \frac{\partial v}{\partial t} + \frac{\partial \lambda_x uv}{\partial x} + \frac{\partial \lambda_y vv}{\partial y} + \frac{\partial \lambda_z wv}{\partial z} = -\frac{\gamma_v}{\rho}\frac{\partial p}{\partial x} + \frac{\partial}{\partial x}\left\{\gamma_x v_e \left(\frac{\partial v}{\partial x} + \frac{\partial u}{\partial y}\right)\right\} \tag{3}$$

$$+\frac{\partial}{\partial y}\left\{\gamma_y v_e \left(2\frac{\partial v}{\partial y}\right)\right\} + \frac{\partial}{\partial z}\left\{\gamma_z v_e \left(\frac{\partial v}{\partial z} + \frac{\partial w}{\partial y}\right)\right\} - \gamma_v D_y v - R_y + \gamma_v S_u$$

$$\lambda_v \frac{\partial w}{\partial t} + \frac{\partial \lambda_x uw}{\partial x} + \frac{\partial \lambda_y vw}{\partial y} + \frac{\partial \lambda_z ww}{\partial z} = -\frac{\gamma_v}{\rho}\frac{\partial p}{\partial y} + \frac{\partial}{\partial x}\left\{\gamma_x v_e \left(\frac{\partial w}{\partial x} + \frac{\partial u}{\partial z}\right)\right\} \tag{4}$$

$$+\frac{\partial}{\partial y}\left\{\gamma_y v_e \left(\frac{\partial w}{\partial y} + \frac{\partial z}{\partial z}\right)\right\} + \frac{\partial}{\partial z}\left\{\gamma_z v_e \left(2\frac{\partial w}{\partial z}\right)\right\} - \gamma_v D_z w - R_z + \gamma_v S_u - \frac{\gamma_v \rho * g}{\rho}$$

$$\gamma_v \frac{\partial F}{\partial t} + \frac{\partial \gamma_x uF}{\partial x} + \frac{\partial \gamma_x vF}{\partial y} + \frac{\partial \gamma_z wF}{\partial z} = S_F \tag{5}$$

Where t was the time, x and y were the horizontal coordinates, z was the vertical coordinate, u, v, w were the velocity components in the x, y and z directions respectively. ρ was the density of the fluid, ρ^* was the relative density of the fluid, p was the pressure. v_e was the kinematic viscosity (the sum of molecular kinematic viscosity and eddy kinematic viscosity), g was the gravitational acceleration, γ_v was the porosity, γ_x, γ_y, γ_z were the real porosity in x, y and z projections. S was the source of mass for wave generation, S_x, S_y, S_z were the momentum sources in x, y, z directions respectively, D_x, D_y, D_z were the coefficient for energy damping in the x, y, z. The next step was to track the interfaces by solving an advection equation, for the function, F, in time series.

The three-dimensional advection equation for fractional function was given as Eq. (5) where S_F was the source of F due to the wave source method. The sharp gradient of VOF function F needed to be conserved at the surface; otherwise, the interface between air and water would lose its definition.

2.2. Numerical Wave Flume

Fig. 1.a and Fig. 1.b showed the longitudinal profile and the plane view of typical beach in Southern Java Island. Fig.1 showed a sandy beach with 30m to 60m in width that can be seen along Lampon village. There is a vegetation area after sandy beach. The width of vegetation area is about 60m to 120m. The hollow topography is located between vegetation and residential areas and the hollow topography has length of 120m, width of 20 m and depth of 2m. Fig. 1.b showed a sandy beach and grass area with 100m to 150m in width that can be seen along Telengria beach in Pacitan. The width of vegetation area is about 60m to 120m after sandy beach. According to the configuration of coastal topography on Lampon village and Pacitan city, this study set the numerical wave flume as shown in Fig. 2. The flume had 750m in length and 34.0 m in height. The offshore wave depth was maintained at 5 m as shown in the upper figure of Fig. 2. A uniform sea bottom slope with 1/25 was set in the flume, and hollow topography was also set on a flat section.

Table 1 showed the list of numerical experiments conducted in this study. Eight cases consisted of two groups; in group 1, there were Case-2, 3, and 4, while in group 2, there were Case-5, 6, 7 and 8. Case-1 had a simple slope without any special topography. The effectiveness of vegetation belts investigated in group 1. In the vegetation cases, the vegetation belts had two variants in width of 100 and 200m, and the density of trees was nine trees/100 m^2 (distance between tree was 5 meters). Case-4 was the case which was similar to Lampoon topography. Case-5 was the single hollow topography, where the width of hollow topography was 100m. Case-6 and 7 were the single combination of hollow and embankment topography, where the Case-6 was hollow topography which set on the seaside of the vegetation belts and the Case-7 was the vegetation belts which set on the seaside of hollow topography. Numerical experiments of Case-8 investigated the combination case of double hollows and double of vegetation belts.

Table 1 List of numerical simulations in this study

No	Cases	width of veg	width of hollow
1	Simple slope	-	-
2	Vegetation	100	-
3	Vegetation	200	-
4	Lampon	150	-
5	Hollow	-	100
6	Vegetation + Hollow (front)	100	100
7	Vegetation + Hollow (back)	100	100
8	2 Vegetation + 2 Hollow	2 x 100	2 x 100

According to the report of tsunami height which was observed in Lampon village (Tsuji et al, 1995) and based on the height of inundation on the landward from the local government (Bappeda Pacitan, 2002), this study generated a bore type tsunami with 6 m in height. This bore wave would generate inundation depth of about 5.5 m on the landward.

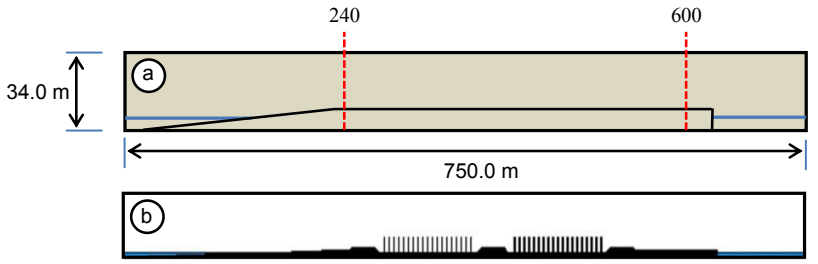

Fig. 2(a) Schematic of numerical flume; (b) snapshot of numerical simulation result (Case-8)

CADMAS-SURF/3D requires time history of water surface elevation and fluid velocity on an input boundary to generate waves with arbitrary profile. This study assumed the bore profile on the offshore region at first and the velocity profile related to this bore profile was obtained by utilizing the following equation **[8]**.

$$U = \frac{C\zeta}{H} = \zeta \sqrt{\frac{g(H+h)}{2H(H-\eta\zeta)}} \tag{6}$$

In this equation, U meant the depth averaged velocity and g meant the gravity acceleration. H=h+ζ meant the total depth from datum and ζ also meant the temporal bore height. η was a coefficient obtained from the ratio between the initial water depth on a propagation area and the total depth of the propagating bore, and it was set as 1.03 in this study.

3. Analysis and Results

In this study, both water surface elevation and flow velocity were measured at two locations, i.e. 240m and 600m from the input boundary as the reference points in order to evaluate the reduction effect of tsunami inundated flow on the inundation section as shown in Fig. 2.

3.1. Numerical Results Case-1, 2, 3 and 4

Coastal vegetation belts have economic benefits and these benefits can be extended if vegetation belts are planned according to tsunami disaster mitigation. In developing countries, budgets for tsunami hazards are very limited. On the other hand, the existing coastal vegetation does not provide maximum protection from tsunami hazards. Numerical experiments in this group investigated the effectiveness of vegetation belts in reducing inundated flow energy and compared it with the case that is similar to the Lampon case. The important parameter of vegetation cases is the width of the vegetation belt. Fig. 3 and Fig. 4 showed the snapshot of tsunami inundation in Case-3 and Case-4. The results of this group showed that the effect of vegetation belts in reducing the intensity of inundation flow seemed to be small in this study.

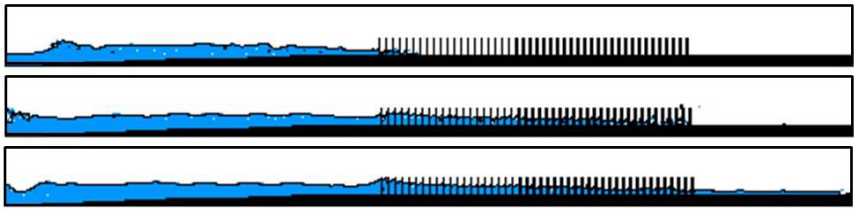

Fig. 3 Snapshot of numerical simulation result in Case-3

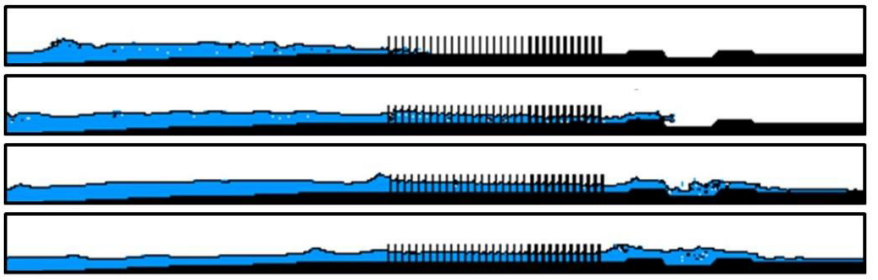

Fig. 4 Snapshot of numerical simulation result in Case-4

Due to the smaller effect of vegetation area on reducing tsunami energy, the water surface profiles and velocity ones in each case seemed to be similar, even when the simulation conducted in different width of vegetation belt setup. Table 2 showed the maximum values of the inundated flow depth and velocity obtained from the profiles in Fig. 5 and Fig. 6. In this group, Case-4 had the highest efficiency in reducing inundated flow depth and velocity.

Table 2 Maximum inundated flow and velocity at 240m and 600m location (Case-1, 2, 3 and 4)

Case	wave height (m)		velocity (m/s)	
	240	600	240	600
1	5.50	2.72	5.87	6.92
2	5.50	2.20	5.87	5.98
3	5.50	2.19	5.87	6.11
4	5.50	1.67	5.87	5.20

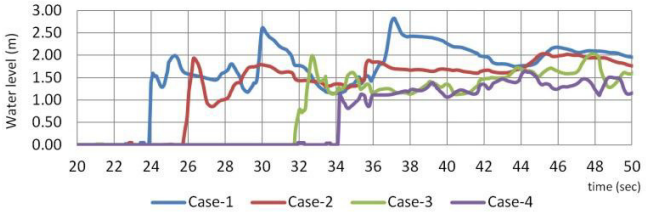

Fig. 5 Profiles of inundated flow depth at 600m location (Case-1, 2, 3 and 4)

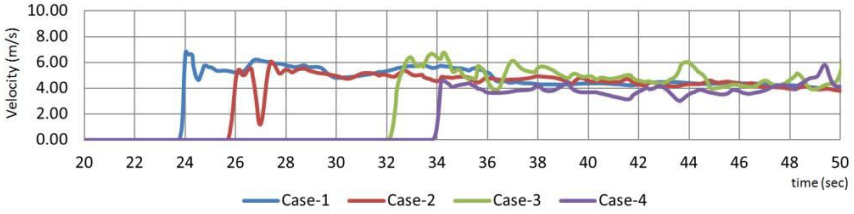

Fig. 6 Profiles velocity at 600m location (Case-1, 2, 3 and 4)

As shown in Case-4, larger flow reflection could be observed in front of the embankment which was set after vegetation and in the hollow topography. It seemed that the topography with embankment and hollow diminished the inundated flow at first, and landward topography reduced the intensity of tsunami inundation again due to the flow reflection significantly. It is clear that the multiple-use of hollow and embankment reduced the inundated water depth and velocity better in comparison with the previous numerical results in cases of vegetation belts.

3.2. Numerical Results Case-1, 5, 6, 7 and 8

Numerical experiments of Case-5 investigated the effectiveness of hollow topography according to the previous one in Lampon Village case.

Table 3 Maximum inundated flow and velocity at 240m and 600m location (Case-1, 5, 6, 7 and 8)

Case	wave height (m)		velocity (m/s)	
	240	600	240	600
1	5.50	2.72	5.87	6.92
5	5.50	1.92	5.87	6.23
6	5.50	1.65	5.87	5.35
7	5.50	1.52	5.87	4.67
8	5.50	1.26	5.87	3.35

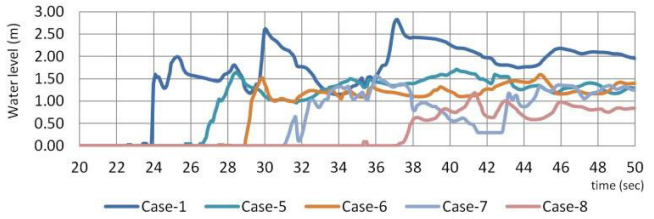

Fig. 7 Profiles of inundated flow depth at 600m location (Case-1, 5, 6, 7 and 8)

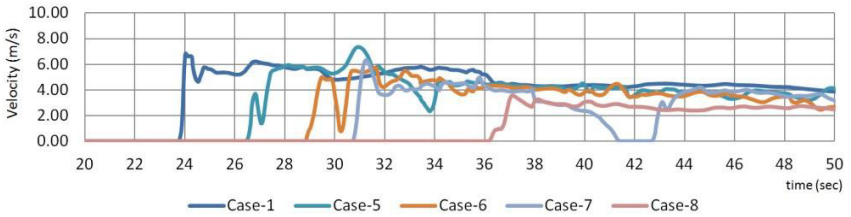

Fig. 8 Profiles velocity at 600m location (Case-1, 5, 6, 7 and 8)

Case-6 and Case-7 investigated the multiple-use of embankment, vegetation and hollow in the case with limitation of land available at coastal area. Case-6 set the combination of topography beside the shoreline and Case-7 before residential area. Case-8 investigated the multiple-use of embankment, vegetation and wider hollow area in reducing inundated flow energy.

The effect of the embankment in reducing the intensity of inundation flow seemed to be better in decreasing water flow and depth. Table 3 showed the maximum values of the inundated flow depth and velocity obtained from the profiles in Fig. 7 and Fig. 8. Fig. 7 showed the water surface profiles and velocity ones at 600m location from Case-5, 6, 7 and 8. Fig.9 and Fig. 10 showed the snapshot of tsunami inundation in Case-5 and Case-8. It is clear that the multiple-use of hollow, vegetation and embankment reduced the inundated water depth and velocity better in comparison with the previous numerical results.

As shown in Fig. 10, larger flow reflection could be observed in front of the embankment which was set between vegetation and hollow topography. It seemed that the topography with embankment and hollow on shore side diminished the inundated flow at first, and landward topography reduced the intensity of tsunami inundation again due to the flow reflection significantly. Case-8 had the highest efficiency in reducing inundated flow depth and velocity in this group. Regarding the limitation of beach width, combination of hollow and embankment topography might be arrayed without eliminating the vegetation belts before the residential area for better trapped effect from the embankment and hollow configuration.

Furthermore, the multiple-use of hollow and embankment extremely shortened the duration of inundation as well. This means that the mass of water inundated into landward might be reduced extremely by the multiple uses of hollow and embankment topography.

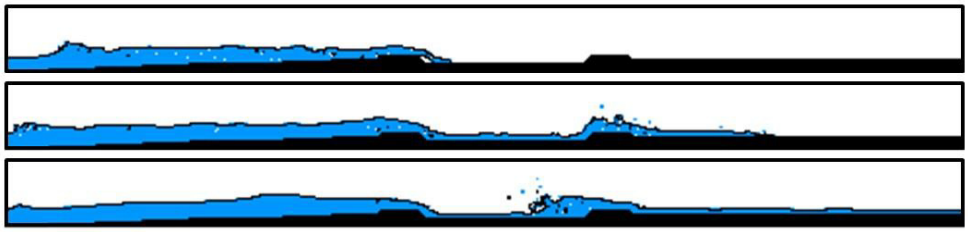

Fig. 9 Snapshot of numerical simulation result in Case-5

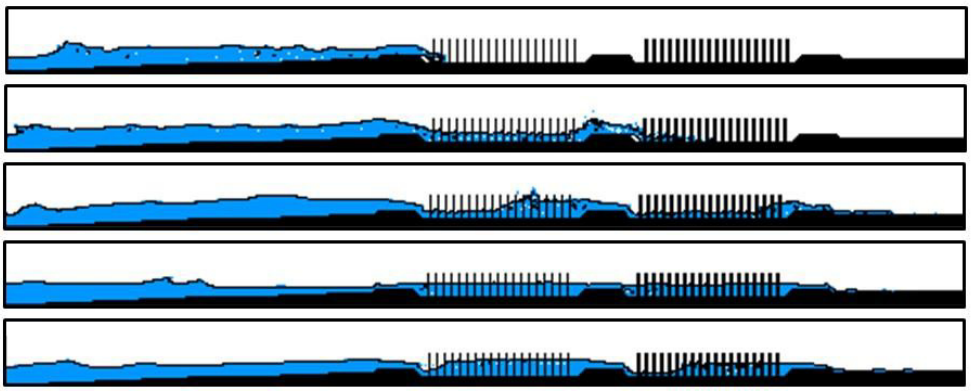

Fig. 10 Snapshot of numerical simulation result in Case-8

4. Horizontal Force due to Inundated Flow

Reduction of the inundated flow depth and velocity led the smaller hydraulic force acting on some structures on landward area. Fig. 11 showed the ratio of hydraulic force caused by the inundation flows in all cases. The index, αi, in this figure meant a ratio of the hydraulic force, and it was defined as $\alpha i = (ui2/hi)/(u12/h1)$. In this equation, i meant a case number, and $u1$ and $h1$ meant the inundated flow velocity and water depth in Case-1 which had a uniform simple slope and flat section.

This study found that trap effect of hollow topography due to tsunami was effective to decrease the horizontal force. These results meant that the use of local wisdom, which was a modification of coastal topography developed in Lampon village, could be one of the favorable countermeasures against tsunami attack. Furthermore, the multiple-use of embankment and hollow topography enhanced the efficiency of reducing hydraulic force as seen in Case-8. Table 4 showed numerical results of wave height (WL), velocity (U) and hydraulic force against inundated flow (α) at 600m measurement point.

Table 4 Numerical results of WL, U and α

Case	WL	U	U2	α
1	2.72	6.92	47.89	1.00
2	2.20	5.98	35.76	0.92
3	2.19	6.11	37.33	0.97
4	1.67	5.20	27.04	0.92
5	1.92	6.23	38.81	1.15
6	1.65	5.35	28.62	0.99
7	1.52	4.67	21.81	0.81
8	1.26	3.35	11.22	0.51

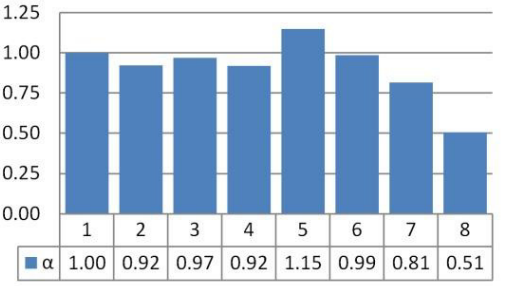

Fig. 11 Ratio of hydraulic force against Case-1

5. Conclusion

This study evaluated the efficiency of topography modification, which was developed in Lampon village, Indonesia as one of the local wisdoms in reducing tsunami energy. This study evaluated the efficiency of other contrivances, such as parallel use of embankment and hollow topography, combination of vegetation area, and a multiple-use of hollow and embankment topography in order to enhance the performance of countermeasures introduced as a local wisdom. This study cleared that the configuration of Lampoon topography had the function of reducing tsunami inundation energy. Case-4 (Lampoon topography) reduced the hydraulic force of about 90% on inundation area in comparison with the case without any measures in Case-1. Furthermore, the parallel use of embankment and hollow topography could enhance the reduction of hydraulic force due to the flow reflection.

The multiple-use of embankment, vegetation and hollow topography extremely lowered the hydraulic force, more than 50%, against the case without any measures. This system also shortened the duration of inundation as well, and the system could check with the mass of water inundate into landward area. Effectiveness of vegetation area on reducing tsunami inundation energy seemed to be very small in this study, according to wide of the vegetation belt. The vegetation area with enough width had the function of reducing tsunami energy, and the parallel use of vegetation area with embankment and hollow topography was better in comparison to the other cases in this study.

References

1. Yanagisawa H, Koshimura S, Goto K, Miyagi T, Imamura F, Ruangrassamee A. The reduction effects of mangrove forest on a tsunami based on field surveys at Pakarang Cape, Thailand and numerical analysis. *Estuary Coast Shelf Science*. 2009; **81(1)**: 27–37.
2. H. Ismail, A. K. Abd Wahab, N. E. Alias.: Determination of mangrove forest performance in reducing tsunami run-up using physical models, *Natural Hazard.* 2012; **63 (2)**: 939–963.
3. Latief, H. and Hadi, S. The role of forests and trees in protecting coastal areas against tsunamis, Coastal protection in the aftermath of the Indian Ocean tsunami: What role for forests and trees? FAO Corporate Documentary Repository, Khao Lak, Thailand. *Food and Agriculture Organization of the United Nation.* 2006
4. Ranasinghe, H. Assessment of Tsunami damage to coastal vegetation & Development of Guidelines for integrated coastal area management, FAO Corporate Documentary Repository, Khao Lak, Thailand. *Food and Agriculture Organization of the United Nations*. 2006
5. Tanaka, N., Sasaki, Y., Mowjood, M.I.M., Jinadasa, K.B.S.N. and Homchuen, S. Coastal vegetation structures and their functions in tsunami protection: experience of the recent Indian Ocean tsunami, *Landscape and Ecological Engineering*. 2007; **3 (1)**: 33-45,
6. Tsuji, Y., Imamura, F., Matsutomi, H., Harada, S., Jumaidi., Arai, K.: Field Survey of the East Java Earthquake and Tsunami of June 3, 1994, *Pure and Applied Geophysics (PAGEOPH)*. 1995; **144 (3/4)**: 839-854.
7. Sakakiyama, T., Kajima, R. Numerical simulation nonlinear waves interacting with permeable breakwaters. Proceedings of the 23rd International Conference on Coastal Engineering, ASCE. 1992; 1517-1530
8. Fukui, Y., S. Hidehiko, M. Nakamura, and Y. Sasaki.: Study on Tsunami, *Annual Journal of Coastal Engineering in Japan*. 1962; **9**: 44-49.